Clim. Past Discuss., 6, 1777–1810, 2010
www.clim-past-discuss.net/6/1777/2010/
doi:10.5194/cpd-6-1777-2010

Climate of the Past Discussions

Sub-millennial climate variability during MIS 11 revealed by high resolution EPICA Dome C isotopic data – a comparison with the Holocene

K. Pol[1], M. Debret[2], V. Masson-Delmotte[1], E. Capron[1], O. Cattani[1], G. Dreyfus[1,3], S. Falourd[1], S. Johnsen[4], J. Jouzel[1], A. Landais[1], B. Minster[1], and B. Stenni[5]

[1]Laboratoire des Sciences du Climat et de l'Environnement, IPSL, CEA CNRS UVSQ UMR 8212, CEA Saclay, L'Orme-des-Merisiers, 91191 Gif-Sur-Yvette Cedex, France
[2]Laboratoire De Morphodynamique Continentale et Côtière – UMR CNRS 6143, Bât IRESE A, Département de Géologie, Université de Rouen, 76821 Mont Saint Aignan Cedex, France
[3]Department of Geosciences, Princeton University, Princeton, NJ, USA

[4]Centre for Ice and Climate, Niels Bohr Institue, University of Copenhagen, Juliane Maries Vej 30, 2100 Copenhagen, Denmark
[5]Università di Trieste, Dipartimento di Scienze Geologiche, Ambientali e Marine, Via E. Weiss 2, 34127 Trieste, Italy

Received: 28 July 2010 – Accepted: 16 August 2010 – Published: 20 September 2010

Correspondence to: K. Pol (katy.pol@lsce.ipsl.fr)

Published by Copernicus Publications on behalf of the European Geosciences Union.

Abstract

We expand here the description of the Antarctic temperature variability during the long interglacial period occurring ~400 thousand years before present (Marine Isotopic Stage, MIS 11). This is achieved thanks to new detailed deuterium measurements conducted on the EPICA Dome C ice core, Antarctica, with a ~50 year temporal resolution. Despite an ice diffusion length reaching ~8 cm at MIS 11 depth, the data allow to highlight a variability at multi-centennial scale for MIS 11, as it has already been observed for the Holocene (MIS 1). Differences between MIS 1 and MIS 11 are analysed regarding the links between multi-millennial trends and sub-millennial variability. The EPICA Dome C deuterium record shows an increased variability and a shift in the observed periodicities at the onset of the final cooling phase of MIS 11, with stronger millennial to multi-millennial variability. Our findings are robust with respect to sensitivity tests on the somewhat uncertain MIS 11 duration.

1 Introduction

Past interglacials, free from human impact on climate, are nowadays well documented thanks to long available climatic records such as marine sediment (Lisiecki and Raymo, 2005) or ice cores (Jouzel et al., 2007; Loulergue et al., 2008; Spahni et al., 2005; Lüthi et al., 2008; Siengenthaler et al., 2005) and offer the possibility to study the natural climate variability during warm periods (Tzedakis et al., 2009). Improving the knowledge of their dynamics is expected to provide a better understanding of the past and future evolution of our present warm climatic period: the Holocene, whose natural course is disturbed by anthropogenic forcings (IPCC, 2007). In this context, the challenge consists to find the most appropriate past interglacial for a comparison with the Holocene. Occurring in an orbital configuration close to the actual one (low eccentricity) around 400 thousands of years ago (hereafter noted ka), Marine Isotope Stage (MIS) 11 was proposed to be a good candidate thanks to a high correlation between the mean 65° N

CPD
6, 1777–1810, 2010

June insolations of MIS 1 (or Holocene) and 11 (Loutre and Berger, 2000, 2003). Although the Antarctic temperature derived from the EPICA Dome C (EDC) isotopic data (Jouzel et al., 2007) exhibits values up to +2 °C higher than the mean value for present day at the MIS 11 maximum (dated around 406 ka using the EDC3 chronology, Parrenin et al., 2007), the concentrations in CO_2 (Siengenthaler et al., 2005) and CH_4 (Spahni et al., 2005) reach similar levels, around 280 ppm and 710 ppb respectively, during MIS 11 and pre-industrial period. Moreover recent sea-level records (Bowen, 2010; Rohling et al., 2010) converge towards an estimation of sea-level at ~400 ka comparable with the actual one, as it was previously suggested by McManus et al. (2003) and Waelbroeck et al. (2002) and modelled by Bintanja et al. (2005).

The climatic contexts of MIS 1 and 11 thus present interesting similarities. However controversies have emerged regarding the orbital alignment of the two interglacials with implications for the prediction of the MIS 1 duration. The debate summarized in Tzedakis (2010) arises from the choice of aligning either precession (Loutre and Berger, 2000, 2003; Ruddimann, 2005, 2007) or obliquity (EPICA-community-members, 2004; Masson-Delmotte et al., 2006) for the synchronisation of the two interglacials. A recent marine study (Dickson et al., 2008) tends to support the alignment of obliquity; nevertheless the double-peak precession configuration of MIS 11 still contrasts with the orbital context of MIS 1 marked by a single precession maximum. A careful comparison with earlier past interglacials now points out MIS 19 as the warm climatic period with the closest orbital configuration to the Holocene one (Pol et al., 2010; Rohling et al., 2010; Tzedakis, 2010). The study of MIS 19 remains difficult due to age scale uncertainties as well as the lack of high resolution records (Pol et al., 2010). Instead, MIS 11 offers the ability to document at high resolution natural climate variability along the longest interglacial recorded since one million years ago and the establishment of the 100 ka glacial-interglacial cycles (Bintanja et al., 2005; Jouzel et al., 2007; Lisiecki and Raymo, 2005).

While earlier comparisons of MIS 11 and Holocene focused on the analysis of their trends or amplitudes (EPICA-community-members, 2004; Masson-Delmotte et al.,

CPD
6, 1777–1810, 2010

2006), we propose here to analyse the Antarctic high frequency climate variability along these two periods. Our study relies on new high resolution measurements of water stable isotope ratios (deuterium/hydrogen ratio expressed as δD) conducted on the EDC ice core, which have improved the temporal resolution for MIS 11 (Sect. 2). The new resolution, close to the Holocene one (~20 years), allows us to compare the sub-millennial climatic variability of these two interglacials through spectral analyses of δD and therefore temperature fluctuations, in relationship with the long term trends. Section 3 is dedicated to the description of the methods before presenting the results (Sect. 4) and the variability analyses (Sect. 5) in detail. Spectral analyses are obviously highly dependent on the age-scale and on the estimation of MIS 11 duration. As differences have been reported between the EDC3 chronology (Parrenin et al., 2007) used in Jouzel et al. (2007) and other age-scales (Kawamura et al., 2010; Lisiecki and Raymo, 2005), we perform sensitivity tests for different MIS 11 durations, compatible with orbital constrains derived from available and new EDC air data records, and discuss the robustness of our variability analyses. At last, we investigate the possible mechanisms at the origin of the observed δD variability during MIS 1 and 11 periods (Sect. 6).

2 Material

The EDC site in East Antarctica (75°06′ S, 123°21′ E) has provided ~3260 m of ice core. A long δD record unveiling ~800 ka of local temperature variations (Jouzel et al., 2007) is available thanks to the measurements of 5800 samples coming from the continuous cut of the core every 55 cm, called "bag samples". In central Antarctica, the climatic information imprinted in surface snow stable isotope composition is affected by post deposition processes such as firn diffusion and wind scouring. Detailed signal to noise studies conducted at Vostok have shown an effective preservation of the climate signal at a temporal resolution of ~20 years (Ekaykin et al., 2002). In EDC, the 55 cm sampling allows to document the Holocene climate variability at this temporal step of

CPD
6, 1777–1810, 2010

~20 years (Masson-Delmotte et al., 2004), but due to ice thinning, describes at a lower temporal resolution past interglacials. A second cut of the EDC core providing 11 cm long samples, called "fine samples" (Pol et al., 2010), increases the depth resolution by a factor of 5, thus improving the temporal resolution for stable isotope records over past interglacials.

Here, the MIS 11 stable isotope variability initially documented with a time resolution of ~220 years by bag δD data (Jouzel et al., 2007) is now accessible at a time resolution of ~45 years thanks to the new high resolution δD measurements, conducted on 770 fine samples between depths of ~2694 and 2779 m. Referring to the threshold of −403‰ as an arbitrary definition of Antarctic warm periods (related to the minimum 300 year average δD value observed over the past ~12 ka, EPICA-community-members, 2004), the MIS 11 warm Antarctic phase is found in the depth interval from ~2699 to 2779 m. This interval is dated between ~395 and 426.7 ka, according to the official time-scale for the EDC core (EDC3 by Parrenin et al., 2007), with an uncertainty of ~6 ka on absolute ages and of ±20% on MIS11 duration (estimated at ~32 ka). Here, we have extended the study up to ~2694 m in order to also depict the glacial inception. The time interval of the study thus ranges from ~392.5 to 426.7 ka.

3 Methods

3.1 Deuterium measurements

The method for deuterium analysis is the same as for the original bag samples measurements. Water is reduced on uranium to form H_2 gas as described in Vaughn et al. (1998) for measuring the fine samples, including ~30% replicate measurements. Data are given with an analytical accuracy of ±0.5‰ at 1σ. The coherency during the MIS 11 period between the bag and fine samples can be checked with the calculation of an averaged signal on 5 fine cut data. The signal derived from the individual bag samples is statically less accurate (0.5‰ at 1σ) than the average signal (±0.23‰ at

CPD
6, 1777–1810, 2010

1σ) which benefits from an experimental noise reduced by a factor of $\sqrt{5}$, thanks to the 5 measurements used for its establishment instead of one for the bag samples profile, over the same 55 cm depth interval.

3.2 Correction for isotopic diffusion

Water stable isotopes undergo firn and ice isotopic diffusion. After snow deposition, such processes gradually smooth isotope profiles by removing the highest frequency climatic information first during the firnification (Johnsen, 1975, or more recently Neumann and Waddington, 2004) and then in the solid ice (Ramseier, 1967). In the upper part of the firn, direct exchanges between snow water molecules and vapour, involving sublimation-condensation processes, erase high frequency isotopic variations. In solid ice, smoothing results from the temperature-dependent molecular diffusivity of water stable isotopes causing self diffusion inside ice crystals.

Diffusion models can be applied to a given ice core to evaluate the smoothing of isotope profiles using the diffusion length σ (characteristic length in cm of an ice layer affected by the smoothing at a given depth), and to reconstruct the original amplitude of climatic variations (back diffused signals). Here we use the Johnsen et al. (2000) method, with the implementation of the parameters suitable for the EDC core (see Pol et al., 2010), on our new δD data. A spectral analysis with respect to depth (cycles/m) of the high resolution signal is performed and the associated red noise of the power spectrum is translated into a diffusion length. This relies on the following equation $A = A_0 \cdot \exp\left(-\frac{1}{2}\sigma^2 \cdot k^2\right)$, which links the amplitude of a given harmonic cycle A recorded in the data and altered by the diffusion within the ice, to the initial amplitude A_0 (with σ the diffusion length and k the wave number associated to the harmonic cycle). The empirical diffusion length at the MIS 11 depth, estimated here to be ~8 cm thanks to our high resolution data, allows to reconstruct the original amplitude of climatic variations recorded in the isotopic signal.

As already mentioned, we cannot expect to preserve climatic information below

CPD
6, 1777–1810, 2010

~20 years in central Antarctica considering post depositional processes (Ekaykin et al., 2002), even though the bag samples are supposed to describe the Holocene at a better temporal resolution (from 8 years at the top of the core to 18 years at ~12 ka depth). The isotopic diffusion occurring in the upper part of the core only affects the part of the signal that is supposed to highlight periodicities lower than 20 years. Therefore the isotopic diffusion is considered insignificant for the Holocene record studied here.

3.3 Variance analysis

To characterize the new information about MIS 11 climatic variability revealed by the high resolution EDC δD data, we first re-sample our signals (the original and the back-diffused ones) on a regular time-step of 50 years. For the comparison between MIS 11 and 1, a 20 year time-step is chosen for the Holocene δD. The long term trends, calculated using a Singular Spectrum Analysis (SSA method) and representing multi-millennial scale climatic variations, are subtracted from the signals to focus on the millennial to sub-millennial scale variability (<5000 years). The variance of the signals is then described using a running standard deviation calculated on the de-trended signals, over 3 ka from the past to the next 1.5 ka at a given time point. This time period is an arbitrary choice for describing the high frequency variability on a millennial scale; it is constrained by the duration of MIS 1 and the temporal resolution available for MIS 11. Other tests have been performed using shorter or longer reference lengths without changing the principal features described in Sect. 5.1. In order to compare the variability with the trends, we have calculated coherently with the running standard deviation a running average of the trends over each 3 ka interval.

3.4 Spectral analysis

To examine the frequency distribution of the isotopic record, we also perform spectral analyses of our re-sampled and de-trended original δD signals. We will not discuss in the next the same analysis on the MIS 11 back-diffused signal as it does not provide

CPD
6, 1777–1810, 2010

any supplementary information on the power spectra. Here we use the wavelet analysis method particularly well adapted for describing non-stationarities or changes in frequency and magnitude (Torrence and Compo, 1998), common characteristics of climatic records. This method (mathematical formalization described in Debret et al., 2007) is used to decompose, for different exploratory scales, a signal in a sum of small wave functions of finite length that are highly localized in time, unlike the classical Fourier transform which explores the complete length of the signal and separates it into infinite-length sine-wave functions. Resulting in a loss of time information, the Fourier analysis thus fails to detect the time variable statistical properties of stochastic processes.

To avoid edge effects and spectral leakage produced by the finite length of the time series, these last ones were zero-padded to twice the data length. However this leads to underestimate the lowest frequencies near the edges of the spectrum. It is thus requested to assess the areas (known as cones of influence) which delineate the parts of the spectrum where estimated energy bands are likely to be less powerful than they actually are. For all local wavelet spectra, Monte Carlo simulations are then used to assess the statistical significance of peaks. The background noise for each signal is firstly separated and estimated using singular spectrum analysis. Secondly an autoregressive modelling is performed for each noise time series to determine the AR(1) stochastic process against which the initial time series has to be tested. The estimated power spectra are here tested against a background white noise (AR(1)=0) and the confidence levels are taken above 95% of this white noise.

4 Results

Figure 1 (panel a) displays the results from our new high resolution δD measurements (black) for MIS 11 depths (from 2694 to 2799 m), confronted to the initial low resolution δD signal (red), published in EPICA-community-members (2004) and in Jouzel et al. (2007). The new high resolution data confirm the general trend exhibited by the

CPD
6, 1777–1810, 2010

red curve. The first Antarctic Isotope Maximum (AIM) event – also exhibited by the CO_2 (Spahni et al., 2005) and CH_4 (Loulergue et al., 2008) records – is observable at ~2775 m. It is followed by a slow warming and a plateau between depths of ~2770 and 2750 m, the maximum of δD being reached at ~2735 m before the beginning of the cooling phase. The comparison over the same 55 cm depth interval between the "calculated" signal (black) derived from high resolution data (see Sect. 3.1) and the previous low resolution profile (red) shows a good agreement over the full period, within their respective accuracy (refer to the Sect. 3.1), and confirms the robustness of the measurements. Differences of 1‰ in average and up to 2‰ can be nevertheless observed during the warming phase, over depth intervals ranging between 2640 and 2646 m or 2660 and 2666 m. In parallel, the new data have been used for the calculation of the EDC δD-excess during MIS 11. The quality of the new high resolution δD measurements is confirmed by stronger correlation with δ^{18}O bag data (not published yet) over the MIS 11 period (R^2=0.98 using the average of the detailed δD data versus 0.97 using the initial bag δD data), as well as by the smaller dispersion with respect to this linear regression (~0.8 versus 1.1‰). This comforts us in the reliability of our new deuterium measurements.

Thereafter we focus on the added information brought by the high resolution δD data, the signal being examined with respect to time. The reference time-scale for the EDC core is the EDC3 chronology established by Parrenin et al. (2007). Figure 1c displays the high resolution δD signal on the corresponding time interval from ~392 to ~427 ka. The signal corrected for isotopic diffusion is shown in grey and exhibits increased variability up to 2‰.

5 Variability analysis: MIS 1 and 11 comparison

Our new δD data for MIS 11 now enable a detailed comparison of climate variability below millennial scale during MIS 1 and 11 thanks to the comparable temporal resolutions of ~45 years and ~20 years, respectively. The Holocene is scrutinized from

CPD
6, 1777–1810, 2010

the present day to 11.7 ka (beginning of the plateau or AIM 1 just after the Antarctic Cold Reversal, Jouzel et al., 1995, 2001); the MIS 11 from 397 to 421 ka, to avoid the difficulty of correctly capturing both the AIM event around ∼425 ka (Fig. 1c) and the abrupt cooling after 397 ka using the SSA method. Panels a of Fig. 2 display the resampled δD signals (initial ones in black and the MIS 11 back diffused one in grey) and the calculated trends (red) over the two interglacials. The signals are centred on their respective mean value, ∼−396‰ for the Holocene and ∼−391‰ for the MIS 11, with a δD difference of 5‰ corresponding to a ∼0.8 °C temperature gradient according to the modern spatial slope of 6‰ per °C (Masson-Delmotte et al., 2008) in East Antarctica. While this modern spatial slope is of current use for interpreting glacial-interglacial changes (Jouzel et al., 2003, 2007), the magnitude of the variability for present-day or warmer conditions may be underestimated (by typically 30%), as suggested by isotope modelling studies for present day interannual variability (Schmidt et al., 2007) or for projections towards a warmer CO_2 world (Sime et al., 2008).

The comparison of the long term trends first allows to characterize the corresponding multi-millennial climate variability (>5000 years) over the two focused periods and to depict two different evolutions. The Holocene exhibits two successive plateaus, one between 10 and 11.7 ka characterized by a δD anomaly of ∼+4‰ and the second one from the present day to 5.5 ka, at the Holocene mean level. In contrast, MIS 11 presents a slow δD increase between 413 and 421 ka followed by a rapid warming that reaches a δD optimum at ∼407 ka of ∼ +2‰ above the MIS 11 mean value level, before finally entering its cooling phase. The relationship between these long term trends and the high frequency climate variability of our two interglacials is then documented by a variance and a spectral analysis, following the methods described in Sects. 3.3 and 3.4.

5.1 Variance analysis

By subtracting the red signal to the black one (Fig. 2 panels a), one can access to the millennial to sub-millennial scale variability as represented on panels b of Fig. 2.

CPD
6, 1777–1810, 2010

The remaining signal gives information on the amplitude of variations characteristic of both periods. Even after the correction for isotopic diffusion (see Sect. 3.2), the MIS 11 δD signal characterized by a maximal amplitude of variations of ~7‰ does not reach the level of variability exhibited during the Holocene one (up to ~10‰). This difference partly arises from the Holocene temporal resolution more than twice higher than for MIS 11. When re-sampling the Holocene every 50 years as done for MIS 11, the amplitude of MIS 1 variation is reduced to 8‰.

In order to go beyond the problem of variability levels, we compare the evolution of sub-millennial climate variability (Fig. 2 panels c) by calculating a running standard deviation over 3 ka of the panels b signals (see Sect. 3.3). The lower variability for MIS 11 is again clearly depicted with values oscillating around 2‰ (up to 2.5‰ after back diffusion correction in grey) against 3.5‰ for MIS 1. For the description of the variability evolution, the noticeable points of standard deviation slope changes are labelled by letters ordered from the past to the present. The Holocene variability first shows a progressive increase of ~0.6‰ from point 1.A to 1.B. Then the variability decreases (until the point 1.C) before reaching a quite stable level (albeit with a weak increase during the last 5 ka). The MIS 11 pattern of variability is characterized by a non-stable area followed by a quickly increasing variability (by 1‰ from 11.A to 11.B) with a maximal running standard deviation value of ~2.5‰ hold until the point 1.C. The variability then decreases by 0.5‰ (from 11.C to 11.D) before progressively increasing again at the end of MIS 11. Except for the overall level of variability, the pattern remains unchanged when taking into account isotopic diffusion (grey curve). Therefore only the original signal (in black) is discussed in the rest of the study.

These changes of millennial to sub-millennial-scale variability can be linked to the long term trend by plotting (panels d Fig. 2) the running standard deviation with respect to a running average over 3 ka of each interglacial δD signal trend. This approach highlights the progressive increase of the Holocene variability (from 1.A to 1.B) occurring during the cooling phase between the two plateaus. In contrast, its decrease until 1.C is linked to the slow Mid-Holocene warming. For MIS 11, the noticeable increase

CPD
6, 1777–1810, 2010

of variability between 11.A and 11.B begins just before the optimum of the δD signal. The highest value of the standard deviation is maintained stable during the beginning of the cooling phase. After an abrupt decrease (from 11.C to 11.D), the variability keeps increasing during the final cooling phase at the end of MIS 11. Despite a symmetrical aspect of the δD trend on each side of the MIS 11 optimum (comparable increasing and decreasing trends), the sub-millennial variability exhibits a clear shift between the warming and the cooling phases. MIS 11 presents thus a higher level of variability during all the cooling phases, even after its abrupt decrease (from 11.C to 11.D). This feature is comparable to the Holocene increasing variability observed during the short cooling between its two plateaus. This highlights a difference in terms of climate dynamics between cooling and warming phases.

5.2 Spectral analysis

We have performed a spectral analysis of the de-trended signals (displayed on Fig. 2 panels b, black) for each interglacial focused period described (Fig. 3) using the wavelets analysis method (see Sect. 3.4). The difference of temporal resolution between MIS 1 and 11 implies a different available range of frequencies for our two interglacial periods (25 to 10 ka^{-1} for MIS 1 and 11, respectively corresponding to 40 and 100 year cycles). For the present comparison we focus on multi-centennial variability which is accessible with the 50 year resolution of MIS 11 data. Due to the diffusion (characterized by a ~8 cm diffusion length at MIS 11 depth, see Sect. 3.2) all the periodicities under ~130 years are lost in the spectral signal. Figure 3 displays the time continuous spectra of the two interglacials.

We can first observe a millennial to multi-centennial scale variability for both interglacials. The Holocene is marked by significant periodicities from 150 to ~300 years punctually present over the full period. The multi-centennial scale variability is less pronounced over the full MIS 11 spectrum with only one significant periodicity of ~500 years detected at ~406 ka (based on EDC3 chronology). At the same time, the millennial scale variability becomes more present with significant periodicities from

CPD
6, 1777–1810, 2010

~1100 to ~1400 years. This transition phase in the MIS 11 variability coincides with the beginning of the cooling phase when regarding the general trend (Fig. 2 panel a). The previous observation of high and increasing amplitudes of variations during this period (after 11.B, see Sect. 5.1) can thus be attributed to the onset of millennial variability. The multi-millennial scale variability presents in the same way a major transition at ~406 ka, with a continuous periodicity of ~3400 years present during the first part of the MIS 11 (from ~421 to 406 ka), shifting towards ~2500 years at the end of the period. Altogether these results highlight the establishment of a new mode of climatic variability during the final cooling phase of MIS 11, as firstly noted in the variance analysis. By comparison, a small transition in the MIS 1 millennial scale variability can also be detected at ~5.5 ka with a ~950 year periodicity changing into a ~800 year cycle. This corresponds to the beginning of the second plateau of the Holocene (see Fig. 2 panel a) which is also marked by amplitudes of variations progressively decreasing (segment 1.B to 1.C) before reaching a stable level of variability (Sect. 5.1).

5.3 Sensitivity to uncertainties on MIS 11 duration

The previous comparison between MIS 1 and 11 climate variability features is constrained by their durations, here based on the EDC3 chronology (Parrenin et al., 2007). Referring to the −403‰ level for the definition of an interglacial in the EDC core (see Sect. 2, EPICA-community-members, 2004) the EDC3 age-scale estimates that MIS 1 has lasted ~12 ka so far, consistently with the new EDC chronology established back to 50 ka (Lemieux-Dudon et al., 2010), derived from a new inverse method for ice core dating (Lemieux-Dudon et al., 2009). The estimate for MIS 11 duration is of ~32 ka with a given uncertainty of ±20% (±6.4 ka). With an added difficulty of comparing different type of records that use different references for delineating the interglacial periods, the Lisiecki and Raymo (2005) chronology for marine sediment cores establishes the beginning of MIS 1 at ~11 ka and evaluates the benthic MIS 11 duration of 20 ka between 398 and 418 ka (with an uncertainty of 4 ka on absolute ages), suggesting a shorter MIS 11 than depicted in EDC3 for Antarctic temperature. In parallel,

CPD
6, 1777–1810, 2010

Kawamura et al. (2010) have recently extended an orbital $\delta O_2/N_2$ chronology for the Antarctic Dome Fuji (DF) core, first established for the past 360 ka (Kawamura et al., 2007), back to 470 ka. They obtain a MIS 11 duration shorter by ~9 ka in comparison with the EDC3 chronology. Such differences between MIS 11 length estimates lead us to perform sensitivity tests on MIS 11 duration and evaluate the impacts on MIS 11 climate variability using the same variance and spectral analyses as before (see Sect. 5).

Considering O_2/N_2 ratios measured in trapped air of ice cores as direct tools (free from the usual Δ age between gas and ice) for the establishment of orbital tuning chronology (Bender, 2002), we have used EDC O_2/N_2 unpublished data (Dreyfus et al., 2010) to test two others age scales for MIS 11 (Fig. 1c). By synchronising arbitrary the mean 75° S insolation curve to the EDC O_2/N_2 record (as done in Dreyfus et al., 2010), we produce a first age-scale which shortens our MIS 11 signal by ~4 ka, now dated between 395.2 and 425.7 ka (Fig. 1d, hereafter Test1). Such a reduced duration was also tested in Rohling et al. (2010) and remains within the uncertainty range of the EDC3 time-scale. A second age-scale test can be produced by fitting the EDC3 with the orbital DF chronology, reducing in larger proportions the MIS11 duration by ~8.5 ka, between 400.5 and 426 ka (Fig. 1e, hereafter Test2).

Focusing on the same part of the MIS 11 signal as in Sect. 5, the variability is then analysed on the corresponding reduced time-intervals ranged from 399 to 421.3 ka and from 403.7 to 420 ka for Test 1 and 2 (Fig. 2). The impacts of Test 1 on MIS 11 variability analysis are globally negligible compared to the previous results obtained with the EDC3 age-scale. The amplitude of variations (panel b) is hardly affected; the running standard deviation (panel c) and its evolution with respect to trend (panel d) logically exhibit an overall similar pattern as the one produced using the EDC3 age-sale. By contrast, the significant shortening of the MIS 11 duration by Test 2 drops the level of variability by 1.5‰. The running standard deviation is then affected and presents values of 0.3‰ lower in average than using the original signal. Its evolution with respect to the trend is impacted with less pronounced changes of variability levels

CPD
6, 1777–1810, 2010

(between 11.A and 11.B, 11.C and 11.D, panel d). But both for Test 1 and Test 2, the panels d illustrate that the main features described in Sect. 5.1 remain unchanged, showing that the age-scale uncertainties do not affect our main conclusions regarding changes in variance.

The spectral analysis is more impacted by the reductions of MIS 11 durations (Fig. 3). First, the distinct transition in multi-millennial variability occurring at ~406 ka observed on the EDC3 signal becomes more diffuse with only one significant periodicity of ~3200 years, with Test 1; this periodicity becomes insignificant using Test 2. The MIS 11 pattern of multi-millennial climate variability is clearly affected by uncertainties on MIS 11 duration. Second the significant periodicities at millennial to multi-centennial scale are preserved but with values slightly shifted (~1400 turning into ~960 years and ~500 into ~320 years between EDC3 chronology and Test 2). Altogether, our sensitivity tests confirm the robustness of a changing climate dynamics at the onset of the final MIS 11 cooling phase.

6 Discussion

We now discuss the links between the variability features highlighted in the δD signals of MIS 1 and 11, natural climate forcings and internal climate variability. While long term changes have classically been attributed to the climate system response to orbital forcing, the drivers of millennial to sub-millennial variability involve external forcings such as solar and volcanic activities, as well as internal climate dynamics implying the oceanic and atmospheric components (as further discussed in the following subsections). In particular, one can question the influence of local processes such as precipitation intermittency, moisture origin, evaporation conditions in relationship with atmospheric circulation and austral ocean surface conditions on Antarctic δD records.

As the Holocene benefits from a substantial documentation, we first discuss the results of MIS 1 spectral analysis in the context of available literature. Assuming that the patterns of forcings and internal modes of variability described over the last 12 ka

CPD
6, 1777–1810, 2010

were also at play during MIS 11, we can then suggest that the same mechanisms are involved during MIS 11. However due to the uncertainties on MIS 11 duration which impact the significant periodicities highlighted thanks to our high resolution δD data, the parallel between MIS 1 and 11 climate forcings remains difficult to establish. The discussion is thus limited to the comparison of the general evolutions of MIS 11 δD signal and others climate records from different proxies available for MIS 11 period.

6.1 Spectral Holocene EDC characteristics

By examining the solar activity during the Holocene (as detailed in Steinhilber et al., 2009), we first note that our EDC δD Holocene variance (Fig. 2, panels c) cannot simply be explained by changes in solar variability and deserves the exploration of others climate forcings. Spectral analyses of the EDC δD signal during Holocene have already been performed (Yiou et al., 1997; Masson et al., 2000) but without clearly examining the possible relationships with climate actors. Here the wavelet method presents the advantage to mark the onset of the significant periodicities of the Holocene EDC δD signal. Then, they can be compared to the results of many previous studies that have discussed millennial to multi-centennial Holocene variability and its signature in different climate and solar activity records.

The implication of solar forcing in the millennial scale variability of Holocene has been first supported by Bond et al. (1997, 2001). Thanks to cosmogenic nucleides (^{14}C and ^{10}Be) measurements, they indeed claimed that the Holocene 1500-year (±500) periodicity found in North Atlantic drift ice records can be attributed to solar forcing. The same periodicity has also been detected in other proxies of the North Atlantic region (Bianchi and McCave, 1999; Campbell et al., 1998; Mayewski et al., 1997 as a non-exhaustive list), as in the South Hemisphere (Lamy et al., 2001), but without underlining a persistent link with solar activity. Using a wavelet analysis method on several records from the North Hemisphere, Debret et al. (2007) actually highlights a decoupling of the apparent Holocene 1500-year climatic cycle into three superimposed significant periodicities of 1000, 1500 and 2500 years. Whereas the comparison of different

CPD
6, 1777–1810, 2010

marine sediment cores (Bianchi and McCave, 1999; Chapman and Shackleton, 2000; Giraudeau et al., 2000) preferentially attributes the ~1500-year periodicity to oceanic dynamics, the link between 1000 and 2500-year climatic cycles and solar activity is confirmed when confronting the spectral analyses of Bond et al. (2001) records and of the Vonmoos et al. (2006) ^{10}Be data.

Exhibiting cyclicities close to ~1000 years, our EDC Holocene δD record (Fig. 3) could also corroborate the solar forcing at millennial scale in the Antarctic region. However the spectral analysis actually highlights a decoupling of the ~1000-year cycle into a ~950-year periodicity during the early Holocene (similar to the Northern records of Bond et al., 2001 and Vonmoos et al., 2006 according to the Debret et al., 2007 analysis and close to the 900-year cycle of Lamy et al., 2001 in the South), to a ~850-year one in the late Holocene (also recorded in Chapman and Shackleton, 2000). This transition phase in the frequency domain, recorded at ~5.5 ka in our EDC δD signal and phasing with the establishment of a progressive stable level of variability (see Sect. 5.2), has already been documented in Debret et al. (2009), in a synthesis of records covering the two Hemispheres. The transition phase known as Mid-Holocene transition, is suggested by the authors to underline a change in the dominant mechanisms of variability, from an external origin (essentially from solar activity) in the early Holocene, to internal processes in the late Holocene. The emergence of two periodicities at ~230 and ~290 years (Fig. 3) at this ~5.5 ka point supports the establishment of a new mode of variability during the Holocene, even at multi-centennial scale. This leads us to now explore the Holocene multi-centennial variability and discuss the possible mechanisms (internal and/or external) at play in the second part of the Holocene.

The multi-centennial variability recorded in the Holocene EDC δD signal is a common feature of both Northern and Southern Hemisphere records. In particular our periodicity of ~230 years has also been found in the East Antarctica sector (Crosta et al., 2007) and is comparable to the ~240-year cycle of the Rousse et al. (2006) data from a North Icelandic marine sediment core, identified in the last 6 ka. Climate models (Park and Latif, 2008; Schulz et al., 2007) indeed show that the multi-centennial

CPD
6, 1777–1810, 2010

variability is a persistent feature of Atlantic Ocean circulation. Park and Latif (2008) have demonstrated the implication of both hemispheres in high frequency variability through large changes in the Atlantic sea ice extent, with a rapid response of the Northern Hemisphere at decadal scale and a slower one of the Southern Hemisphere at multi-centennial scale.

Invoking a sun-ocean-climate linkage, Hu et al. (2003) underline the possible forcing of the multi-centennial changes in sea ice extent by the centennial solar forcing (Karlén and Kuylenstierna, 1996). The same forcing is further proposed by Varma et al. (2010) to drive the southern annular mode. Altogether, these studies suggest that the multi-centennial scale variability found in the EDC δD record could be closely associated with changes in austral sea ice extent and atmospheric circulation, in response to multi-centennial variations in solar activity. Changes in volcanic forcing may also be at play (Castellano et al., 2005), as recent modelling studies suggest a possible centennial response time (Stenchikov et al., 2009; Schneider et al., 2009) but have not so far been explored due to the lack of quantitative reconstructions beyond the last millennium (Gao et al., 2008).

However centennial variability may not necessarily be driven by external forcings and may also result from modes of internal climate variability. Modelling experiments focusing on North Atlantic Deep Water (NADW) formation (Jongma et al., 2007; Renssen et al., 2007) have indeed highlighted that internal periodic processes such as freshwater releases could provide a sensible mechanism to explain the Holocene multi-centennial scale variability. Focusing on the thermohaline structure of the Southern Ocean, Pierce et al. (1995) also linked modelled centennial-scale oscillations with changes both in the local precipitation affecting the Antarctic Circumpolar Current and in the NADW.

Thus, while bipolar see-saw patterns are well known to link Antarctica and Greenland stable isotope records during abrupt glacial (Blunier et al., 1998) or early interglacial events (Masson-Delmotte et al., 2010), even at sub-millennial scale (Capron et al., 2010), these modelling experiments reinforce the hypothesis of a similar

CPD
6, 1777–1810, 2010

interhemispheric linkage at play at multi-centennial variability during interglacial periods. Such internal mechanisms could be involved in the observed variability changes at Mid-Holocene transition, as previously suggested by Debret et al. (2009).

6.2 MIS 11 EDC variability

Here the spectral analysis of MIS 11 cannot be discussed in the same way as for MIS 1, due to large uncertainties on MIS 11 duration and the absence of information about external forcings (solar and volcanic activities) for this period. The MIS 11 still benefits from sufficient documentation to allow comparisons between our new EDC δD profile and others proxy signals.

In addition to the various climatic information provided by the EDC core (e.g., Jouzel et al., 2007; Siengenthaler et al., 2005; Spahni et al., 2005), MIS 11 has been documented in other long marine or continental records through different proxies (Lisiecki and Raymo, 2005; McManus et al., 2003; Tzedakis et al., 2006). They consistently underline the general comparable background climate conditions between MIS 1 and 11 (sea level, greenhouse gas concentrations, local temperatures, vegetation history ...) and the exceptional length of MIS 11. One study (de Vernal and Hillaire-Marcel, 2008) emphasizes an exceptional development of boreal ecosystems on the Greenland coasts, suggesting particularly reduced Greenland ice sheet extent during this interglacial. But due to the lack of a sufficient temporal resolution for performing reliable spectral analysis, comparisons with these records remain restricted to the analyses of trends or intensities.

Still, similarities between the EDC CO_2 (Siengenthaler et al., 2005) and the 500 year resolution $\delta^{13}C$ record of a marine core from the Cape Basin (Dickson et al., 2008) at the end of MIS 11 have revealed an interesting oceanic circulation–atmospheric CO_2 concentration linkage. The parallel between the observed $\delta^{13}C$ gradient and CO_2 drawdown at the end of MIS 11 supports the hypothesis of a close link between deep austral ocean ventilation and changes in atmospheric greenhouse gas concentrations (Toggweiler, 1999; Hodell et al., 2003). The onset of an increasing

CPD
6, 1777–1810, 2010

variability in our δD record (at ~406 ka) does not coincide with any marked change in the CO_2concentration. However, its phasing with a methane concentration starting to decrease (Loulergue et al., 2008) and the increase of the EDC sea salt sodium flux (Wolff et al., 2010) is robust given age-scale uncertainties. It suggests that the observed increase in EDC δD variability at the end of MIS 11occurs in parallel with: first, an East Antarctica cooling trend; second, an extent of austral sea ice cover associated to a reduced methane production in tropical and boreal wetlands.

Further discussions about the links between the EDC climate variability (derived from our δD data) and ocean circulation variability requires both higher resolution marine records and improved chronologies and synchronization methods. However as a first step in the MIS 11 variability analysis, our data enable to suggest that the increased Antarctic variance and the onset of millennial to sub-millennial variability are intimately linked with the global transition between interglacial and glacial states.

7 Conclusions

Here we have first demonstrated the interest of the EDC high resolution δD measurements for the comparison between MIS 1 and 11 Antarctic climate variability patterns. The new data have permitted a better documentation of MIS 11 variability, going beyond a comparison of trends and intensities. Our study highlights a specific variability pattern during MIS 11, unexpected from the long term Antarctic deuterium trend exhibiting a quite symmetrical evolution on each side of the late MIS 11 optimum (~406 ka according to the EDC3 chronology, Parrenin et al., 2007). The MIS 11 variability characterized by a calculation of a running standard deviation of the de-trended signal shows an enhanced variability starting at the beginning of the cooling phase compared to the lower variability characterizing the preceding warming phase. This change in variance is due to the onset of millennial to sub-millennial variability when entering the cooling phase as identified by a wavelet spectral analysis. These patterns are robust in spite of uncertainties on MIS 11 duration. We are then tempted to compare the spectra

CPD
6, 1777–1810, 2010

of MIS 11 and MIS 1 and attribute the similar scale variability to processes involved in Holocene millennial to multi-centennial variability. The uncertainties about MIS 11 length which impact the values of significant periodicities revealed by the spectral analysis however limit the validity of our conclusions. We stress the need to: first scrutinize the MIS 11 variability with other records e.g. from tropical, temperate and polar regions at sufficient temporal resolution for improving the global documentation of changes in variability along MIS 11; second, reduce uncertainties on the length of MIS 11 by the building of an accurate reference time-scale for the EDC core which will help in the future to precisely specify the MIS 11 variability spectrum.

Acknowledgements. This work is a contribution to the European Project for Ice coring in Antarctica (EPICA), a joint European Science Foundation/European Commission (EU) scientific program, funded by the EU and by national contributions from Belgium, Denmark, France, Germany, Italy, The Netherlands, Norway, Sweden, Switzerland and the UK. It has in particular benefited from the support of ANR PICC and contributes to the ESF HOLOCLIP programme.

The publication of this article is financed by CNRS-INSU.

References

Bender, M. L.: Orbital tuning chronology for the Vostok climate record supported by trapped gas composition, Earth Planet. Sc. Lett., 204, 275–289, 2002.

Bianchi, G. G. and McCave, I. N.: Holocene periodicity in North Atlantic climate and deep-ocean flow south of Iceland, Nature, 397, 515–517, 1999.

CPD

6, 1777–1810, 2010

Bintanja, R., van de Wal, R., and Oerlemans, J.: Modelled atmospheric temperatures and global sea levels over the past million years, Nature, 437, 125–128, 2005.
Blunier, T., Chappellaz, J., Schwander, J., Dallenbäch, A., Stauffer, B., Stocker, T., Raynaud, D., Jouzel, J., Clausen, H. B., Hammer, C. U., and Johnsen, S. J.: Asynchrony of Antarctic and Greenland climate change during the last glacial period, Nature, 394, 739–743, 1998.
Bond, G., Showers, W., Cheseby, M., Lotti, R., Almasi, P., deMenocal, P., Priore, P., Cullen, H., Hajdas, I., and Bonami, G.: A pervasive millennial-scale cycle in the north atlantic Holocene and glacial climates, Science, 278, 1257–1266, 1997.
Bond, G., Kromer, B., Beer, J., Muscheler, R., Evans, M. N., Showers, W., Hoffmann, S., Lotti-Bond, R., Hajdas, I., and Bonani, G.: Persistent solar influence on north Atlantic climate during the Holocene, Science, 294, 2130–2136, 2001.
Bowen, D. Q.: Sea level ~400 000 years ago (MIS 11): analogue for present and future sea-level?, Clim. Past, 6, 19–29, doi:10.5194/cp-6-19-2010, 2010.
Campbell, I. D., Campbell, C., Apps, M. J., Rutter, N. W., and Bush, A. B. G.: Late Holocene ~1500 yr climatic periodicities and their implications, Geology, 26, 471–473, 1998.
Capron, E., Landais, A., Chappellaz, J., Schilt, A., Buiron, D., Dahl-Jensen, D., Johnsen, S. J., Jouzel, J., Lemieux-Dudon, B., Loulergue, L., Leuenberger, M., Masson-Delmotte, V., Meyer, H., Oerter, H., and Stenni, B.: Millennial and sub-millennial scale climatic variations recorded in polar ice cores over the last glacial period, Clim. Past, 6, 345–365, doi:10.5194/cp-6-345-2010, 2010.
Castellano, E., Becagli, S., Hansson, M., Hutterli, M., Petit, J. R., Rampino, M. R., Severi, M., Steffensen, J. P., Traversi, R., and Udisti, R.: Holocene volcanic history as recorded in the sulfate stratigraphy of the European Project for Ice Coring in Antarctica Dome C (EDC96) ice core, J. Geophys. Res., 110, D06114, doi:10.1029/2004jd005259, 2005.
Chapman, M. R. and Shackleton, N. J.: Evidence of 550-year and 1000-year cyclicities in North Atlantic circulation patterns during the Holocene, Holocene, 10, 287–291, 2000.
Crosta, X., Debret, M., Denis, D., Courty, M. A., and Ther, O.: Holocene long- and short-term climate changes off Adélie Land, East Antarctica, Geochem. Geophy. Geosy., 8, Q11009, doi:10.1029/2007gc001718, 2007.
de Vernal, A. and Hillaire-Marcel, C.: Natural variability of Greenland climate, vegetation, and ice volume during the past million years, Science, 320, 1622–1625, doi:10.1126/science.1153929, 2008.
Debret, M., Bout-Roumazeilles, V., Grousset, F., Desmet, M., McManus, J. F., Massei, N., Se-

CPD
6, 1777–1810, 2010

bag, D., Petit, J.-R., Copard, Y., and Trentesaux, A.: The origin of the 1500-year climate cycles in Holocene North-Atlantic records, Clim. Past, 3, 569–575, doi:10.5194/cp-3-569-2007, 2007.

Debret, M., Sebag, D., Crosta, X., Massei, N., Petit, J. R., Chapron, E., and Bout-Roumazeilles, V.: Evidence from wavelet analysis for a mid-Holocene transition in global climate forcing, Quaternary Sci. Rev., 28, 2675–2688, 2009.

Dickson, A. J., Leng, M. J., and Maslin, M. A.: Mid-depth South Atlantic Ocean circulation and chemical stratification during MIS-10 to 12: implications for atmospheric CO_2, Clim. Past, 4, 333–344, doi:10.5194/cp-4-333-2008, 2008.

Dreyfus, G., Landais, A., Capron, E., Pol, K., Loutre, M.-F., Raynaud, D., Lipenkov, V. Y., Masson-Delmotte, V., Jouzel, J., and Leuenberger, M.: On the limits of orbital dating using EPICA Dome C $\delta O_2/N_2$, J. Geophys. Res. Atm., submitted, 2010.

Ekaykin, A. A., Lipenkov, V. Y., Barkov, N. I., Petit, J. R., and Masson-Delmotte, V.: Spatial and temporal variability in isotope composition of recent snow in the vicinity of Vostok Station: implications for ice-corerecord interpretation, Ann. Glaciol., 35, 181–186, 2002.

EPICA-community-members: Eight glacial cycles from an Antarctic ice core, Nature, 429, 623–628, 2004.

Gao, C., Robock, A., and Ammann, C.: Volcanic forcing of climate over the past 1500 years: An improved ice core-based index for climate models, J. Geophys. Res., 113, D23111, doi:10.1029/2008jd010239, 2008.

Giraudeau, J., Cremer, M., Manthé, S., Labeyrie, L., and Bond, G.: Coccolith evidence for instabilities in surface circulation south of Iceland during Holocene times, Earth Planet. Sc. Lett., 179, 257–268, 2000.

Hodell, D. A., Venz, K. A., Charles, C. D., and Ninnemann, U. S.: Pleistocene vertical carbon isotope and carbonate gradients in the South Atlantic sector of the Southern Ocean, Geochem. Geophy. Geosy., 4, doi:10.1029/2002GC000367, 2003.

Hu, F. S., Kaufman, D., Yoneji, S., Nelson, D., Shemesh, A., Huang, Y., Tian, J., Bond, G., Clegg, B., and Brown, T.: Cyclic variation and solar forcing of Holocene climate in the Alaskan Subarctic, Science, 301, 1890–1893, doi:10.1126/science.1088568, 2003.

IPCC: Climate Change 2007 – The Physical Science Basis, Fourth Assessment Report, edited by: Change, I. P. o. C., Cambridge University Press, Cambridge, 1009 pp., 2007.

Johnsen, S. J.: Stable Isotope Homogenization of Polar Firn and Ice, from the International Symposium on Isotopes and Impurities in Snow and Ice, Proceedings IU66 Symposium 118,

CPD
6, 1777–1810, 2010

210–219, 1977.
Johnsen, S. J., Clausen, H. B., Cuffey, K. M., Hoffmann, G., Schwander, J., and Creyts., T.: Diffusion of stable isotopes in polar firn and ice: the isotope effect in firn diffusion, Physics of ice core records, Hokkaido University Press, 121–140, 2000.
Jongma, J. I., Prange, M., Renssen, H., and Schulz, M.: Amplification of Holocene multicentennial climate forcing by mode transitions in North Atlantic overturning circulation, Geophys. Res. Lett., 34, L15706, doi:10.1029/2007gl030642, 2007.
Jouzel, J., Vaikmae, R., Petit, J. R., Martin, M., Duclos, Y., Stiévenard, M., Lorius, C., Toots, M., A., M. M., Burckle, L. H., Barkov, N. I., and Kotlyakov, V. M.: The two-step shape and timing of the last deglaciation in Antarctica, Clim. Dynam., 11, 151–161, 1995.
Jouzel, J., Masson, V., Cattani, O., Falourd, S., Stievenard, M., Stenni, B., Longinelli, A., Johnsen, S. J., Steffenssen, J. P., Petit, J. R., Schwander, J., Souchez, R., and Barkov, N. I.: A new 27 Ky high resolution East Antarctic climate record, Geophys. Res. Lett., 28, 3199–3202, 2001.
Jouzel, J., Vimeux, F., Caillon, N., Delaygue, G., Hoffmann, G., Masson-Delmotte, V., and Parrenin, F.: Magnitude of the isotope-temperature scaling for interpretation of central Antarctic ice cores, J. Geophys. Res., 108, 1029–1046, 2003.
Jouzel, J., Masson-Delmotte, V., Cattani, O., Dreyfus, G., Falourd, S., Hoffmann, G., Minster, B., Nouet, J., Barnola, J. M., Chappellaz, J., Fischer, H., Gallet, J. C., Johnsen, S., Leuenberger, M., Loulergue, L., Luethi, D., Oerter, H., Parrenin, F., Raisbeck, G., Raynaud, D., Schilt, A., Schwander, J., Selmo, E., Souchez, R., Spahni, R., Stauffer, B., Steffensen, J. P., Stenni, B. S., T. F., Tison, J. L., Werner, M., and Wolff, E.: Orbital and millenial Antarctic climate variability over the past 800 000 years, Science 317, 793–796, 2007.
Karlén, W. and Kuylenstierna, J.: On solar forcing of Holocene climate: evidence from Scandinavia, Holocene, 6, 359–365, 1996.
Kawamura, K., Parrenin, F., Lisiecki, L., Uemura, R., Vimeux, F., Severinghaus, J. P., Hutterli, M. A., Nakazawa, T., Aoki, S., Jouzel, J., Raymo, M. E., Matsumoto, K., Nakata, H., Motoyama, H., Fujita, S., Goto-Azuma, K., Fujii, Y., and Watanabe, O.: Northern Hemisphere forcing of climatic cycles in Antarctica over the past 360 000 years, Nature, 448, 912–915, 2007.
Kawamura, K., Aoki, S., and Nakazawa, T.: Accurate chronology of the Dome Fuji ice core based on O_2/N_2 ratio of trapped air, PAGES 3rd open Science Meeting, Corvalis, OR, USA, 2010.

CPD
6, 1777–1810, 2010

Lamy, F., Hebbeln, D., Röhl, U., and Wefer, G.: Holocene rainfall variability in southern Chile: a marine record of latitudinal shifts of the Southern Westerlies, Earth Planet. Sc. Lett., 185, 369–382, 2001.
Lemieux-Dudon, B., Parrenin, F., and Blayo, E.: A probalistic method to construct an optimal ice chronology for ice cores, Phys. Ice Core Records, II, 68, 2009.
Lemieux-Dudon, B., Blayo, E., Petit, J.-R., Waelbroeck, C., Svensson, A., Ritz, C., Barnola, J.-M., Narcisi, B. M., and Parrenin, F.: Consistent dating for Antarctic and Greenland ice cores, Quaternary Sci. Rev., 29, 8–20, doi:10.1016/j.quascirev.2009.11.010, 2010.
Lisiecki, L. E. and Raymo, M. E.: A Pliocene-Pleistocene stack of 57 globally distributed benthic δ^{18}O records, Paleoceanography, 20, doi:10.1029/2004PA001071, 2005.
Loulergue, L., Schilt, A., Spahni, R., Masson-Delmotte, V., Blunier, T., Lemieux, B., Barnola, J. M., Raynaud, D., Stocker, T., and Chappelaz, J.: Orbital and millenial-scale features of atmospheric CH_4 over the last 800 000 years, Nature, 453, 383–386, 2008.
Loutre, M. F. and Berger, A.: Future climatic changes: are we entering an exceptionally long interglacial?, Clim. Change, 46, 61–90, 2000.
Loutre, M. F. and Berger, A.: Marine isotope stage 11 as an analogue for the present interglacial, Global Planet. Change, 36, 209–217, 2003.
Lüthi, D., Floch, M. L., Bereiter, B., Blunier, T., Barnola, J. M., Siegenthaler, U., Raynaud, D., Jouzel, J., Fischer, H., Kawamura, K., and Stocker, T. F.: High resolution carbon dioxide concentration record 650 000–800 000 years before present, Nature, 453, 379–382, 2008.
Masson-Delmotte, V., Stenni, B., Blunier, T., Cattani, O., Chappellaz, J., Cheng, H., Dreyfus, G., Edwards, R. L., Falourd, S., Govin, A., Kawamura, K., Johnsen, S. J., Jouzel, J., Landais, A., Lemieux-Dudon, B., Lourantou, A., Marshall, G., Minster, B., Mudelsee, M., Pol, K., Röthlisberger, R., Selmo, E., and Waelbroeck, C.: Abrupt change of Antarctic moisture origin at the end of Termination II, P. Natl. Acad. Sci. USA, 107(27), 12091–12094, doi:10.1073/pnas.0914536107, 2010.
Masson-Delmotte, V., Stenni, B., and Jouzel, J.: Common millenial scale variability of Antarctic and Southern Ocean temperatures during the past 5000 years reconstructed from EPICA Dome C ice core, The Holocene, 14, 145–151, 2004.
Masson-Delmotte, V., Dreyfus, G., Braconnot, P., Johnsen, S., Jouzel, J., Kageyama, M., Landais, A., Loutre, M.-F., Nouet, J., Parrenin, F., Raynaud, D., Stenni, B., and Tuenter, E.: Past temperature reconstructions from deep ice cores: relevance for future climate change, Clim. Past, 2, 145–165, doi:10.5194/cp-2-145-2006, 2006.

CPD
6, 1777–1810, 2010

Masson-Delmotte, V., Hou, S., Ekaykin, A., Jouzel, J., Aristarain, A., Bernardo, R. T., Bromwhich, D., Cattani, O., Delmotte, M., Falourd, S., Frezzotti, M., Gallée, H., Genoni, L., Isaksson, E., Landais, A., Helsen, M., Hoffmann, G., Lopez, J., Morgan, V., Motoyama, H., Noone, D., Oerter, H., Petit, J. R., Royer, A., Uemura, R., Schmidt, G. A., Schlosser, E., Simões, J. C., Steig, E., Stenni, B., Stievenard, M., Broeke, M. v. d., Wal, R. v. d., Berg, W.-J. v. d., Vimeux, F., and White, J. W. C.: A review of Antarctic surface snow isotopic composition: observations, atmospheric circulation and isotopic modelling, J. Climate, 21, 3359–3387, 2008.

Masson, V., Vimeux, F., Jouzel, J., Morgan, V., Delmotte, M., Ciais, P., Hammer, C., Johnsen, S., Lipenkov, V. Y., Mosley-Thompson, E., Petit, J.-R., Steig, E., Stievenard, M., and Vaikmae, R.: Holocene climate variability in Antarctica based on 11 ice cores isotopic records, Quaternary Res., 54, 348–358, 2000.

Mayewski, P. A., Meeker, L. D., Twickler, M. S., Whitlow, S., Yang, Q., Lyons, W. B., and Prentice, M.: Major features and forcing of high-latitude northern hemisphere atmospheric circulation using a 110 000-year-long glaciochemical series, J. Geophys. Res., 102, 26345–26366, doi:10.1029/96jc03365, 1997.

McManus, J. F., Oppo, J., Callen, J., and Healey, S.: Marine Isotope Stage 11 (MIS 11): Analog for Holocene and future climate?, Geoph. Monog. Series, 137, 69–85, 2003.

Neumann, T. A. and Waddington, E. D.: Effects of firn ventilation on isotopic exchange, J. Glaciol., 169, 183–194, 2004.

Park, W. and Latif, M.: Multidecadal and multicentennial variability of the meridional overturning circulation, Geophys. Res. Lett., 35, L22703, doi:10.1029/2008gl035779, 2008.

Parrenin, F., Barnola, J.-M., Beer, J., Blunier, T., Castellano, E., Chappellaz, J., Dreyfus, G., Fischer, H., Fujita, S., Jouzel, J., Kawamura, K., Lemieux-Dudon, B., Loulergue, L., Masson-Delmotte, V., Narcisi, B., Petit, J.-R., Raisbeck, G., Raynaud, D., Ruth, U., Schwander, J., Severi, M., Spahni, R., Steffensen, J. P., Svensson, A., Udisti, R., Waelbroeck, C., and Wolff, E.: The EDC3 chronology for the EPICA Dome C ice core, Clim. Past, 3, 485–497, doi:10.5194/cp-3-485-2007, 2007.

Pierce, D. W., Barnett, T. P., and Mikolajewicz, U.: Competing roles of heat and freshwater flux in forcing thermohaline oscillations, J. Phys. Oceanogr., 25, 2046–2064, 1995.

Pol, K., Masson-Delmotte, V., Johnsen, S., Bigler, M., Cattani, O., Durand, G., Falourd, S., Jouzel, J., Minster, B., Parrenin, F., Ritz, C., Steen-Larsen, H. C., and Stenni, B.: New MIS 19 EPICA Dome C high resolution deuterium data: hints for a problematic preservation of

CPD
6, 1777–1810, 2010

climate variability in the “oldest ice”, Earth Planet. Sc. Lett., doi:10.1016/j.epsl.2010.07.030, 2010.
Ramseier, R. O.: Self-diffusion of tritium in natural and synthetic ice monocrystals, J. Appl. Phys., 38, 2553–2556, 1967.
Renssen, H., Goosse, H., and Fichefet, T.: Simulation of Holocene cooling events in a coupled climate model, Quaternary Sci. Rev., 26, 2019–2029, 2007.
Rohling, E. J., Braun, K., Grant, K., Kucera, M., Roberts, A. P., Siddall, M., and Trommer, G.: Comparison between Holocene and Marine Isotope Stage-11 sea-level histories, Earth Planet. Sc. Lett., 291, 97–105, 2010.
Rousse, S., Kissel, C., Laj, C., Eiríksson, J., and Knudsen, K. L.: Holocene centennial to millennial-scale climatic variability: Evidence from high-resolution magnetic analyses of the last 10 cal kyr off North Iceland (core MD99-2275), Earth Planet. Sc. Lett., 242, 390–405, 2006.
Ruddiman, W. F.: The early anthropogenic hypothesis: Challenges and responses, Rev. Geophys., 45, RG4001, doi:10.1029/2006rg000207, 2007.
Ruddimann, W.: Cold climate during the closest stage 11 analog to recent millennia, Quaternary Sci. Rev., 24, 1111–1121, 2005.
Schmidt, G. A., Legrande, A., and Hoffmann, G.: Water isotope expressions of intrinsic and forced variability in a coupled ocean-atmosphere model, J. Geophys. Res., 112, doi:10.1029/2006JD007781, 2007.
Schneider, D. P., Ammann, C. M., Otto-Bliesner, B. L., and Kaufman, D. S.: Climate response to large, high-latitude and low-latitude volcanic eruptions in the Community Climate System Model, J. Geophys. Res., 114, D15101, doi:10.1029/2008jd011222, 2009.
Schulz, M., Prange, M., and Klocker, A.: Low-frequency oscillations of the Atlantic Ocean meridional overturning circulation in a coupled climate model, Clim. Past, 3, 97–107, doi:10.5194/cp-3-97-2007, 2007.
Siengenthaler, U., Stocker, T. F., Monnin, E., Lüthi, D., Schwander, J., Stauffer, B., Raynaud, D., Barnola, J.-M., Fischer, H., Masson-Delmotte, V., and Jouzel, J.: Stable carbon cycle-climate relationship during the last Pleistocene, Science, 310, 1313–1317, 2005.
Sime, L. C., Tindall, J. C., Wolff, E. W., Connolley, W. M., and Valdes, P. J.: Antarctic isotopic thermometer during a CO_2 forced warming event, J. Geophys. Res., 113, D24119, 10.1029/2008jd010395, 2008.
Spahni, R., Chappellaz, J., Stocker, T. F., Loulergue, L., Hausammann, G., Kawamura, K.,

CPD
6, 1777–1810, 2010

Flückiger, J., Schwander, J., Raynaud, D., Masson-Delmotte, V., and Jouzel, J.: Variations of atmospheric methane and nitrous oxide during the last 650 000 years from Antarctic ice cores, Science, 310, 1317–1321, 2005.
Steinhilber, F., Beer, J., and Fröhlich, C.: Total solar irradiance during the Holocene, Geophys. Res. Lett., 36, L19704, doi:10.1029/2009gl040142, 2009.
Stenchikov, G., Delworth, T. L., Ramaswamy, V., Stouffer, R. J., Wittenberg, A., and Zeng, F.: Volcanic signals in oceans, J. Geophys. Res., 114, D16104, doi:10.1029/2008jd011673, 2009.
Toggweiler, J. R.: Variation of atmospheric CO_2 by ventilation of the ocean's deepest water, Paleoceanography, 14, 571–588, doi:10.1029/1999pa900033, 1999.
Torrence, C. and Compo, G. P.: A practical guide to wavelet analysis, B. Am. Meteorol. Soc., 79, 61–78, 1998.
Tzedakis, P. C., Hooghiemstra, H., and Pälike, H.: The last 1.35 million years at Tenaghi Philippon: revised chronostratigraphy and long-term vegetation trends, Quaternary Sci. Rev., 25, 3416–3430, 2006.
Tzedakis, P. C., Raynaud, D., McManus, J. F., Berger, A., Brovkin, V., and Kiefer, T.: Interglacial diversity, Nat. Geosci., 2, 751–755, 2009.
Tzedakis, P. C.: The MIS 11 – MIS 1 analogy, southern European vegetation, atmospheric methane and the "early anthropogenic hypothesis", Clim. Past, 6, 131–144, doi:10.5194/cp-6-131-2010, 2010.
Varma, V., Prange, M., Lamy, F., Merkel, U., and Schulz, M.: Solar-forced shifts of the Southern Hemisphere Westerlies during the late Holocene, Clim. Past Discuss., 6, 369–384, doi:10.5194/cpd-6-369-2010, 2010.
Vaughn, B., White, J. W. C., Delmotte, M., Trolier, M., Cattani, O., and Stievenard, M.: An automated system for the uranium reduction method of hydrogen isotope analysis of water, Chem. Geol., 152, 309–319, 1998.
Vonmoos, M., Beer, J., and Muscheler, R.: Large variations in Holocene solar activity: Constraints from ^{10}Be in the Greenland Ice Core Project ice core, J. Geophys. Res., 111, A10105, doi:10.1029/2005ja011500, 2006.
Waelbroeck, C., Labeyrie, L., Michel, E., Duplessy, J. C., McManus, J. F., Lambeck, K., Balbon, E., and Labracherie, M.: Sea-level and deep water temperature changes derived from benthic foraminifera isotopic records, Quaternary Sci. Rev., 21, 295–305, 2002.
Wolff, E. W., Barbante, C., Becagli, S., Bigler, M., Boutron, C. F., Castellano, E., de Angelis, M.,

CPD
6, 1777–1810, 2010

Federer, U., Fischer, H., Fundel, F., Hansson, M., Hutterli, M., Jonsell, U., Karlin, T., Kaufmann, P., Lambert, F., Littot, G. C., Mulvaney, R., Röthlisberger, R., Ruth, U., Severi, M., Siggaard-Andersen, M. L., Sime, L. C., Steffensen, J. P., Stocker, T. F., Traversi, R., Twarloh, B., Udisti, R., Wagenbach, D., and Wegner, A.: Changes in environment over the last 800 000 years from chemical analysis of the EPICA Dome C ice core, Quaternary Sci. Rev., 29, 285–295, 2010.

Yiou, P., Fuhrer, K., Meeker, L. D., Jouzel, J., Johnsen, S., and Mayewski, P. A.: Paleoclimatic variability inferred from the spectral analysis of Greenland and Antarctic ice-core data, J. Geophys. Res., 102, 26441–26454, 1997.

CPD
6, 1777–1810, 2010

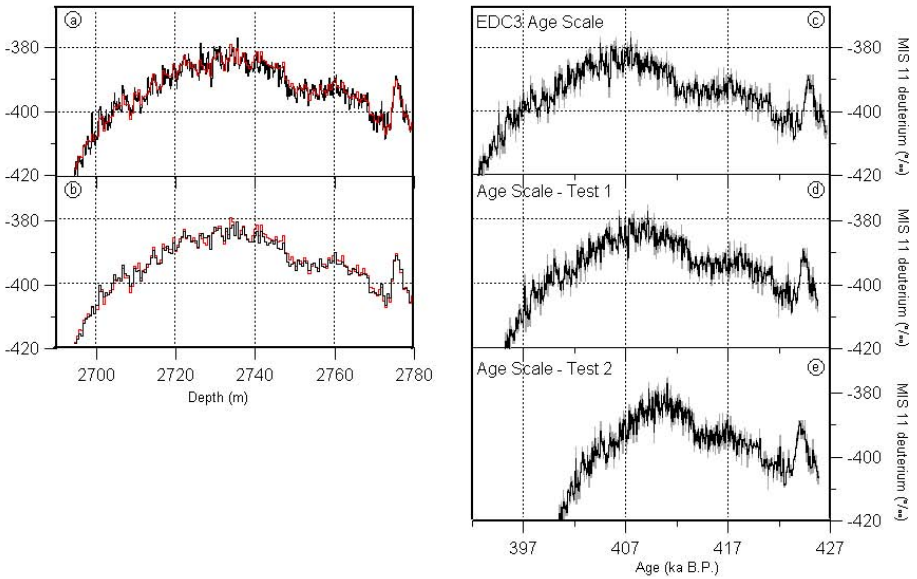

Fig. 1. Summary of the available EDC δD (‰) data for MIS 11 first plotted in function of depth (panels a and b, in m) and then in function of time (panels c to e, in ka). **(a)** δD from MIS 11 bag samples (red) and the new high resolution δD signal from the fine samples (black). **(b)** MIS 11 δD bag samples (red) in comparison with the mean signal (black) obtained from the average of 5 fine cuts. **(c)** High resolution δD data (black) plotted with respect to the official EDC chronology (EDC3, Parrenin et al., 2007) and corrected from the isotopic diffusion (grey). Panels **(d)** and **(e)** display the same signals using two other age-scales (Sect. 5.3) (Test 1 and Test 2, respectively) for sensitivity tests on MIS 11 duration (not shown).

CPD
6, 1777–1810, 2010

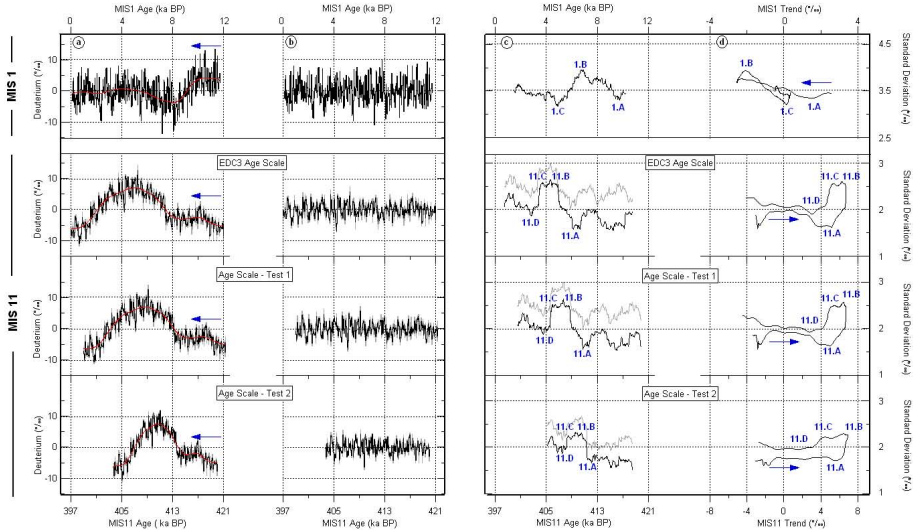

Fig. 2. Continues on the next page.

CPD
6, 1777–1810, 2010

Fig. 2. Variability analysis (in ‰) of MIS 1 (top), MIS 11 using EDC3 chronology (middle top), Test 1 age-scale (middle bottom) and Test 2 age-scale (bottom). **(a)** Signals (black) centred on the δD mean value of the focused period: 0–12 ka for MIS 1; 397–421 ka for MIS 11-EDC3; 399–421.3 ka for MIS 11 – Test1; 403.7–420 for MIS 11 – Test 2. The general trends are plotted in red; signals corrected from isotopic diffusion in grey for MIS 11. **(b)** Signals minus their respective trends (red, panels a). **(c)** Calculated running standard deviation of panel b signals over 3 ka, from the past 1.5 ka to the next 1.5 ka at a given time point (black: original signals; grey: correction for isotopic diffusion). The remarkable changes of slope are labelled from A to C or D from past to present (the 1 or 11 numbers refer to the studied interglacial). **(d)** Running standard deviation (panels c, ‰) plotted in function of the respective general trends (panels a, red, ‰). Signals are smoothed using a binomial algorithm for an easier readability. The labelled points (panels c) are reported and arrows indicate the way of reading from past to present. It has to be noted here that, given the normal distribution of the deuterium variability, the significance of variance changes can be assessed using a Fischer F-test. Significance thresholds differ for the MIS 1 (149 degrees of freedom over 3 ka intervals) and MIS 11 (59 degrees of freedom). At the 95% confidence level, ratios of standard deviations are significant when they are larger than 15% (MIS 1) and 22% (MIS 11). The main changes in variance described previously can therefore be considered as significant.

CPD
6, 1777–1810, 2010

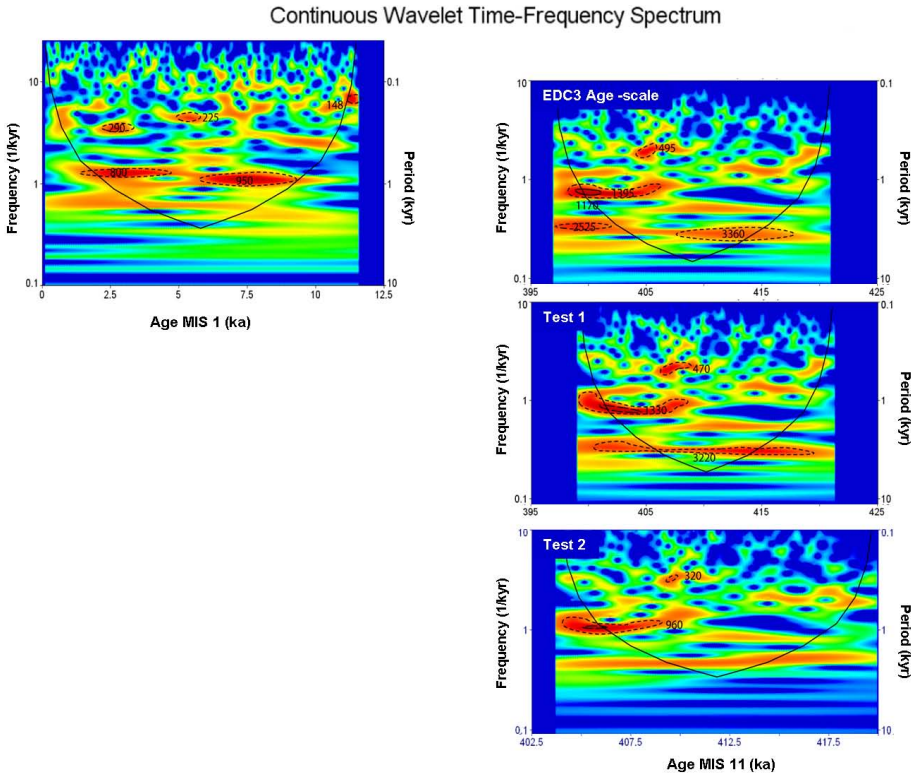

Fig. 3. Spectral analysis of the de-trended signals (displayed on Fig. 2, panels b) for MIS 1 (left) and MIS 11 (right), using EDC3 chronology (top), Test 1 age-scale (middle) and Test 2 (bottom). The spectral power is displayed in function of time (ka) in term of frequency (1/ka, left axis) or period (ka, right axis). Black lines correspond to the cone of influence; dot lines indicate the confidence levels.

CPD
6, 1777–1810, 2010